Orbit response matrix analysis of ATF optics, April 2008

A. Wolski[*]

University of Liverpool, and the Cockcroft Institute, Daresbury, UK.

K. Kubo, S. Kuroda, T. Okugi

KEK, Tsukuba, Ibaraki, Japan.

M.D. Woodley

Stanford Linear Accelerator Center, Menlo Park, California 94025, USA.

(Dated: May 2, 2008)

An analysis of the ATF damping ring optics based on measurements of the orbit response matrix and dispersion is presented. In particular, we aim to determine skew quadrupole settings that may help to reduce the vertical emittance. It is found that the vertical emittance in the fitted model has some sensitivity to certain parameters in the fit parameters, in particular to the weight given to the vertical dispersion. With a relatively low weight on the vertical dispersion, the fitted model has a vertical emittance of around 20 pm, which is broadly consistent with recent measurements of the vertical emittance. We also compare fits based on data from all BPMs in the ATF damping ring, with fits based on data from Echotek BPMs only; the improved quality of the fit to the data in the case of using only Echotek BPMs suggests that these BPMs have very good performance.

I. INTRODUCTION

Previously, efforts to minimize the coupling in the KEK-ATF using an analysis based on the measured orbit response matrix (ORM) [1] have met with partial success [2]. With recent work to upgrade the BPM system [3], and the need to reduce the vertical emittance to allow studies of ion effects and for operation of ATF2, it was felt appropriate to make a further attempt to reduce the vertical emittance using this technique.

ORM analysis is used routinely at a number of light sources, including SPEAR3 [4], the ALS [5] and, more recently, the Australian Synchrotron [6]. Briefly, the technique allows many important machine parameters, including normal and skew quadrupole magnet strengths, BPM gains and couplings, and orbit corrector kicks and tilts, to be determined from measurements of the closed orbit response to changes in strength of orbit corrector magnets. Starting with a model of the machine, the parameters of interest are varied until the orbit response matrix of the model matches as closely as possible the measured orbit response matrix. Since the orbit response matrix typically contains many more elements than the number of parameters used in the fit, the fit is generally highly over-constrained. Therefore, it can be assumed that if a good quality fit is obtained, the fitted model provides a good representation of the real machine.

For previous work at the ATF [2], and for the present studies, we have used the code LOCO (Linear Optics from Closed Orbit) [7] to perform the fit of the machine model to the measured orbit response matrix. LOCO runs within MatLab, and uses the Accelerator Toolbox [8] as the modeling code.

Vertical emittance in a storage ring is generated by vertical dispersion and by betatron coupling. In the ATF, the dominant sources of both of these sources of vertical emittance is believed to be vertical beam offset in the sextupoles. Each sextupole is fitted with skew quadrupole trim windings to compensate any vertical beam offset. Minimization of the vertical emittance therefore requires: first, steering the beam to minimize any vertical offset in the sextupoles; second, adjusting the skew quadrupole strengths to compensate any residual vertical offset, as well as the effects of quadrupole tilts. It is hoped that the optimum steering may be determined by beam-based alignment (BBA) [9]. ORM analysis may then help to determine the optimum skew quadrupole strengths for minimum vertical emittance.

The general procedure for applying ORM analysis to reduce the vertical emittance is as follows. After steering based on BBA results, a machine model is fitted to measured ORM data. The model includes no information on magnet alignment or orbit distortion; and only includes coupling sources at the location of the skew quadrupole magnets used for coupling correction. If a good fit is obtained, particularly to those data related to the betatron coupling and vertical dispersion, then it is assumed that the observed coupling and vertical dispersion are effectively generated by the fitted skew quadrupole strengths. Therefore, changing the skew quadrupole strengths by the negative of the strengths determined in the fit, should correct the observed coupling. The relevant parts of the orbit response matrix for this process are the "cross-plane" components, i.e. the horizontal BPM response to changes in vertical corrector magnet strength, and the vertical BPM response to changes in horizontal corrector magnet strength. It should be noted that the fit to the ORM data generally includes BPM gains and corrector magnet tilts, so that "fake" coupling, appearing from the instrumentation rather than the beam dynamics, does

---

[*]Electronic address: `a.wolski@dl.ac.uk`

not affect the skew quadrupole strengths determined by the fit. This technique has been found to be effective in previous studies at the ATF [2] and in achieving ultra-low emittance in the ALS [5].

In this report, we present the ORM analysis of data collected at the ATF on 3 April, 2008. No attempt has yet been made to correct the coupling in the ATF based on the results of the ORM analysis.

II. FITTING PARAMETERS AND FIT QUALITY

LOCO provides great flexibility in the choice of machine parameters used as variables to fit the model to the measured ORM data. For the analysis presented here, we used the following machine parameters:

- gains and couplings for all functioning BPMs;

- strengths and tilts for all functioning orbit corrector magnets;

- strengths of "discrete" quadrupoles (i.e. not the quadrupole gradient in the main dipoles);

- strengths of skew quadrupoles located at the sextupoles.

For the skew quadrupoles, we investigated both the use of all 68 skew quadrupoles in the fit, and then the use of only those skew quadrupoles on the SF1R sextupoles (i.e. omitting the skew quadrupoles on the SD1R sextupoles, giving 34 skew quadrupoles remaining). The reason for this, is that within each arc cell, the SF1R and SD1R sextupoles are close together, and approximately degenerate in terms of the coupling generated by a beam offset in each sextupole. Therefore, in fitting a skew quadrupole component in these magnets, it can happen that the fit gives large skew quadrupole gradients that approximately cancel in adjacent pairs of sextupoles. By omitting one sextupole in each arc cell, a more "stable" fit is obtained, which can be of almost as good quality as a fit in which every available skew quadrupole is included. Unless otherwise stated, results presented here are for fits using 34 skew quadrupoles (on the SF1R magnets).

BPM gain and coupling parameters are treated independently. Thus, if (x_{meas}, y_{meas}) are the horizontal and vertical beam positions recorded by a BPM for a beam at actual position (x, y), we can write:

$$\begin{pmatrix} x_{meas} \\ y_{meas} \end{pmatrix} = \begin{pmatrix} g_{xx} & g_{xy} \\ g_{yx} & g_{yy} \end{pmatrix} \cdot \begin{pmatrix} x \\ y \end{pmatrix} \qquad (1)$$

where g_{xx} and g_{yy} are the horizontal and vertical gains respectively (ideally taking values $g_{xx} = g_{yy} = 1$); and g_{xy} and g_{yx} parameterise the coupling (ideally, $g_{xy} = g_{yx} = 0$). The values of all four parameters g_{xx}, g_{xy}, g_{yx} and g_{yy} are fitted independently by LOCO. If the BPM "coupling" is the result of a physical tilt of the BPM

buttons, then the four parameters will form a rotation matrix; however, the general situation is that the actual values are determined by effects in the electronics, and not by a physical rotation of the buttons.

The initial model used for fitting was constructed using values for the quadrupole strengths determined from the control system. The skew quadrupoles were turned off in the initial model.

The measured response matrix included data returned from:

- 91 horizontal and 91 vertical BPMs (i.e. all BPMs except numbers 47, 50, 54, 56, 59);

- 47 horizontal orbit corrector magnets (i.e. all horizontal correctors except ZH100R, ZH101R and ZH102R);

- 50 vertical orbit corrector magnets (i.e. all vertical correctors except ZV100R).

The BPMs and corrector magnets that did not return valid data were deemed "not functioning" for the purpose of the analysis.

The fitting routine is based on singular value decomposition of a matrix representing the change in the orbit response matrix to changes in the variables used in the fit. A lower tolerance in excluding singular values potentially gives a better fit; but a tolerance that is too low can mean that large changes in the variables are made to make small improvements in the fit. For the fits used in the present analysis, a tolerance of 5×10^{-6} was generally used, meaning that any singular values less than 5×10^{-6} times the largest singular value were excluded. In practice, this meant excluding less than 5% of the singular values.

Note that with 182 BPMs and 97 correctors, the total number of constraints in the fit (based on measurements of the orbit response matrix and the horizontal and vertical dispersion) is 17,836. With a gain and coupling on each BPM and each orbit corrector magnet, 100 normal quadrupole gradients and 34 skew quadrupole gradients, the number of variables in the fit is 692. Thus, the number of constraints is significantly larger than the number of variables, and the fit is highly over-constrained, as desired.

Fig. 1 indicates the effectiveness of the fitting process by plotting the residuals between the measured and modelled orbit response matrices, for both the initial model, and a fitted model. For clarity, the standard deviations of the residuals along rows (corresponding to different BPMs) and columns (corresponding to different corrector magnets) are plotted. The fit reduces the residuals by one or two orders of magnitude.

The overall quality of the fit can be characterized by the distribution of the residuals between the components of the measured orbit response matrix and the orbit response matrix of the fitted model. If the residuals are normalised to the resolution of the correspdonding BPM, then for a "good" fit, a gaussian distribution of rms width
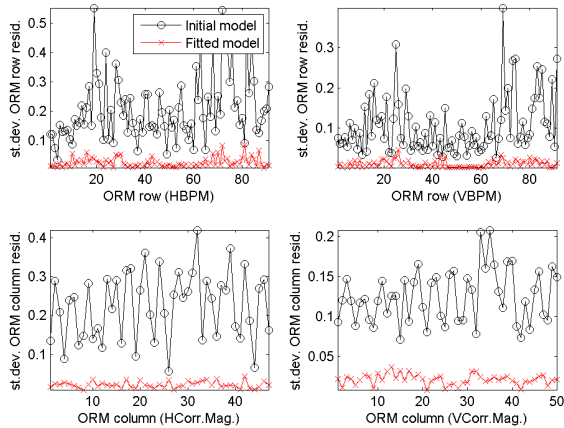
FIG. 1: Quality of the fit of the model to the measured orbit response matrix. The plots show the standard deviation of the residuals along different rows (BPMs) and columns (corrector magnets) of the orbit response matrix. Black circles: residuals for the initial model. Red crosses: residuals for the fitted model.
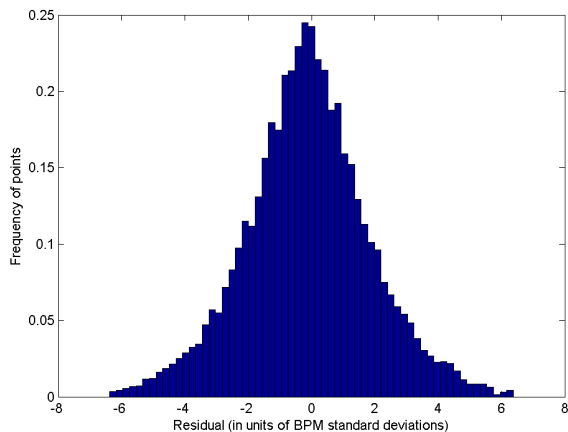

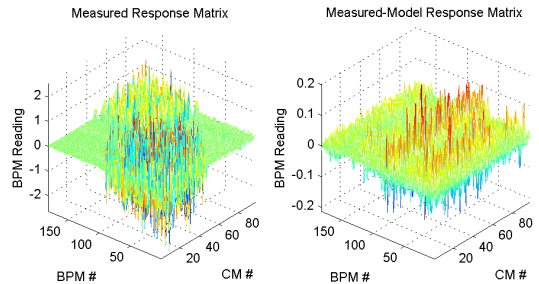FIG. 2: Distribution of residuals from the fit.

FIG. 3: Measured orbit response matrix, and residuals to the fit using 34 skew quadrupoles. Note the difference in vertical scale on the two plots.
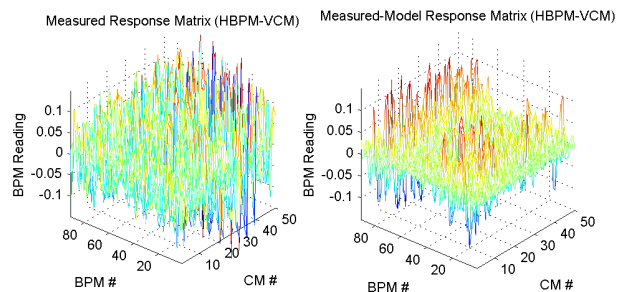

FIG. 4: Coupling sector (horizontal BPM response to vertical orbit corrector magnets) of the measured orbit response matrix, and residuals to the fit using 34 skew quadrupoles.

1 is expected. For the present data, the resolutions of the BPMs were estimated from the raw orbit data, by taking the standard deviation of multiple measurements with fixed orbit corrector settings. For the fit results reported here, the distribution of residuals has a half-width of a little over 2, in units of the BPM resolution ($\chi^2/N \approx 4.5$ where N is the number of degrees of freedom in the fit).

The distribution of residuals for a fit using 34 skew quadrupoles is shown in Fig. 2. Using 68 skew quadrupoles results in a marginal improvement in the fit quality, at the expense of significantly larger fitted gradients on the skew quadrupoles.

The measured orbit response matrix and the residuals to a fit using 34 skew quadrupoles are shown in Fig. 3. The sectors of the orbit response matrix corresponding to betatron coupling are of particular significance when

trying to minimize the vertical emittance. These sectors are shown in Figs. 4 and 5.

The horizontal and vertical dispersions were also measured and used as constraints in the fit. The dispersion was measured in the usual way, by recording the change in orbit resulting from a change in frequency of the rf cavities. It is important to note that this is not the true dispersion, since the measurement is affected by BPM gain and coupling errors; since the gain and coupling errors are simultaneously determined in the fit, they are taken into account in the use of the measured "dispersion" as a constraint. This is particularly important in the vertical plane, since the vertical dispersion is a significant source of vertical emittance, so an accurate determination of the vertical dispersion is necessary for emittance reduction; but with a large horizontal dispersion, even small BPM coupling errors can lead to significant contamination in
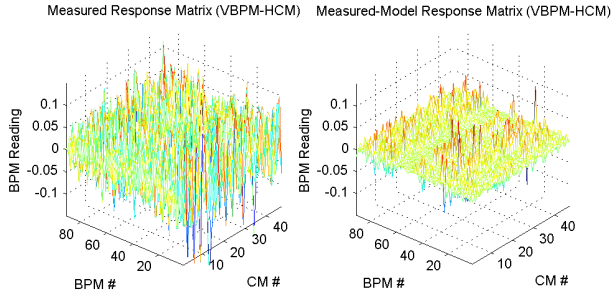
FIG. 5: Coupling sector (vertical BPM response to horizontal orbit corrector magnets) of the measured orbit response matrix, and residuals to the fit using 34 skew quadrupoles.
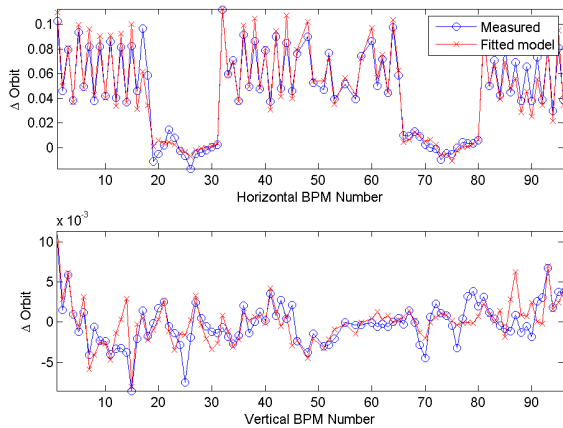

FIG. 7: Quadrupole gradients in the fitted model (red crosses), compared to those in the initial model (black circles).

FIG. 6: Fit to "dispersion" measurement data. Note that the vertical axis is the measured orbit response at the BPMs resulting from a change to rf frequency; this includes effects of BPM gain and coupling errors. In the fit, the horizontal and vertical dispersion were each given a weight of 10.

the measurement of vertical dispersion.

Fig. 6 shows the result of the fit in respect of the measured orbit response to a change in rf frequency. In using LOCO, it is possible to adjust weights given to the dispersion data when making the fit. The fit algorithm treats the dispersion as an additional column in the orbit response matrix (the corresponding "corrector magnet" in this case is the rf frequency); the weight is simply a factor applied to the dispersion measurements before adding them to the orbit response matrix. For the results presented here, we used a weight of 10 for both the horizontal and vertical dispersion data. Increasing the weight on the vertical dispersion data in particular results in an improved fit to these data, but the quality of the fit to the orbit response matrix deteriorates. This
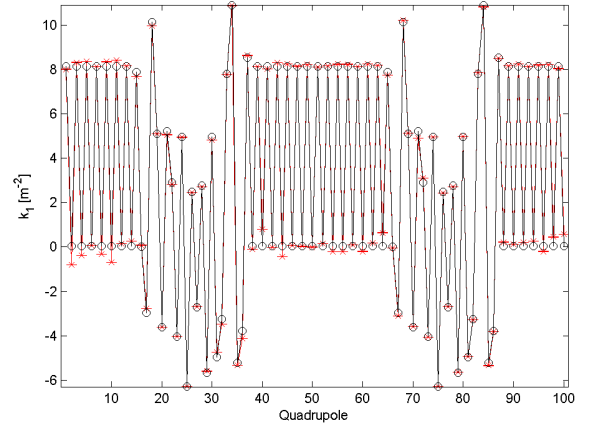
may be an indication that significant vertical dispersion is being generated in the machine by vertical steering, which is not included in the model. In the model, the only sources of vertical dispersion are the skew quadrupoles, which couple dispersion from the horizontal plane into the vertical plane.

III. QUADRUPOLE GRADIENTS AND LATTICE FUNCTIONS

If, given the quality of the fit, one accepts the fitted model as a reasonable representation of the machine, one can compare the fitted model to the initial model determined by the magnet settings read from the control system.

Fig. 7 shows the quadrupole gradients in the fitted model compared with those in the initial model. Figs. 8 and 9 show the horizontal and vertical beta functions respectively, in the initial and fitted models. In each case, we see that there is a beta-beat of about 20% in the fitted model, compared with the initial model. However, there is little variation in the betatron tunes, as can be seen from Table I.

We note that the beta functions determined from the fitted model are not consistent with recent direct measurements of the beta functions, performed by observing the variation in betatron tunes with quadrupole strength [10, 11]. The reasons for the discrepancies are not clear.

Fig. 10 shows the dispersion in the fitted model, compared to that in the initial model. The rms vertical dispersion in the fitted model is 2.7 mm
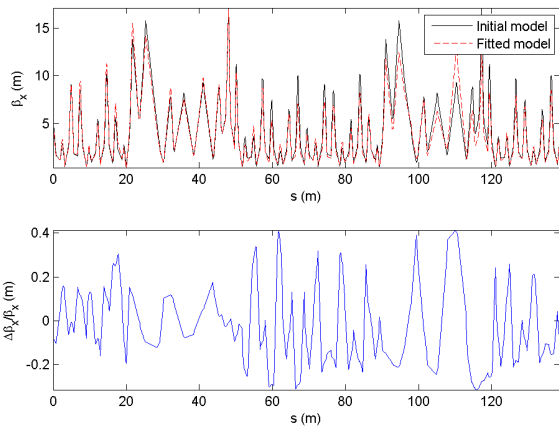
FIG. 8: Horizontal beta function in the fitted model, compared with that in the initial model.
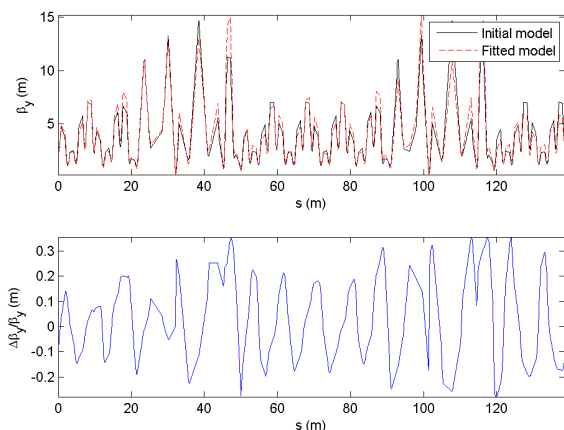

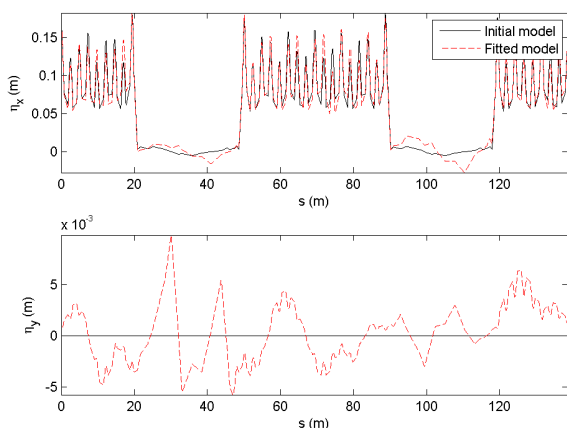FIG. 9: Vertical beta function in the fitted model, compared with that in the initial model.

FIG. 10: Dispersion in the fitted model, compared with that in the initial model. Note that in the initial model, the vertical dispersion is zero everywhere.

model	horizontal tune	vertical tune
initial	15.1825	8.5569
fitted	15.1825	8.5574

TABLE I: Betatron tunes in the fitted model compared with those in the initial model.
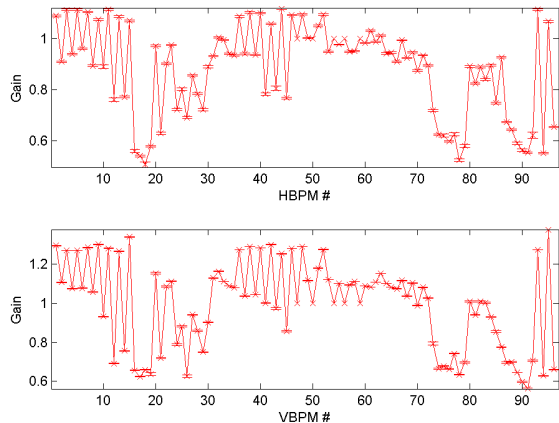

FIG. 11: BPM gains. Top: horizontal gain, g_{xx}. Bottom: vertical gain, g_{yy}. Note that in the initial model, both horizontal and vertical gain are equal to 1.

IV. BPM AND CORRECTOR MAGNET PARAMETERS

The BPM gains and couplings determined from the fitted model are shown in Figs. 11 and 12 respectively. It is interesting to compare the BPM gains determined from the orbit response matrix analysis with recent measurements of BPM response to orbit bumps of known amplitude [12]. The results appear broadly consistent, in terms of the magnitude of the gains, and the locations of BPMs with gains much smaller than 1. A detailed comparison of the two sets of results has not yet been performed.

The orbit corrector magnet strengths are shown in Fig. 13. The "strength" is the change in corrector magnet field strength (in arbitrary units) used when measuring the orbit response matrix. It can be seen that for both horizontal and vertical planes, the kick strengths determined from the fit are systematically weaker than the nominal kick strengths applied in the measurement. The reasons for this are unclear.

It should be noted that for a fit based only on a measured orbit response matrix, there is a degeneracy between an overall factor on the BPM gains, and an overall factor on the corrector strengths (the same orbit response matrix would be obtained if the gain on each BPM was increased by 10%, if the strength of each corrector magnet was simultaneously reduced by 10%). However, this degeneracy is generally resolved by the dispersion measurement, which is independent of the orbit correctors.
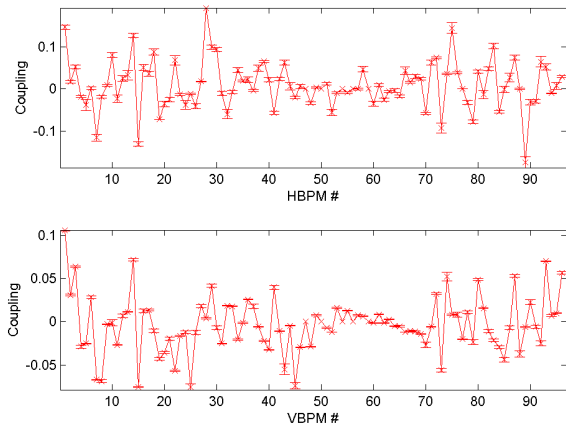
FIG. 12: BPM couplings. Top: coupling g_{xy}. Bottom: coupling g_{yx}. Note that in the initial model, both couplings are equal to 0.
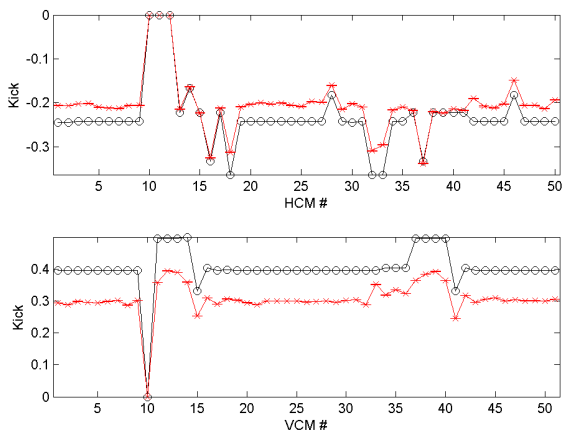

FIG. 13: Corrector strengths in the fitted model (red crosses) compared to the strengths in the initial model (black circles).
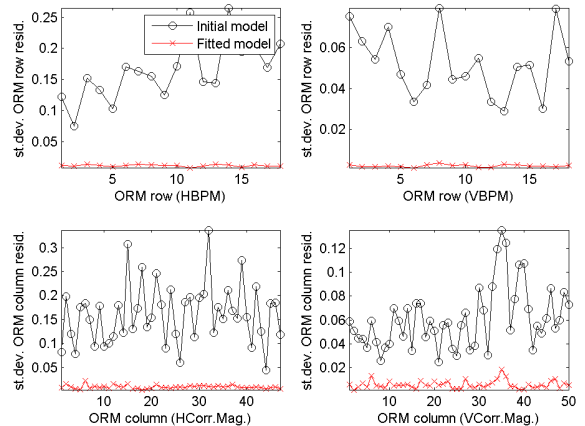

FIG. 14: Quality of the fit of the model to the measured orbit response matrix, using data from Echotek BPMs only. The plots show the standard deviation of the residuals along different rows (BPMs) and columns (corrector magnets) of the orbit response matrix. Black circles: residuals for the initial model. Red crosses: residuals for the fitted model.
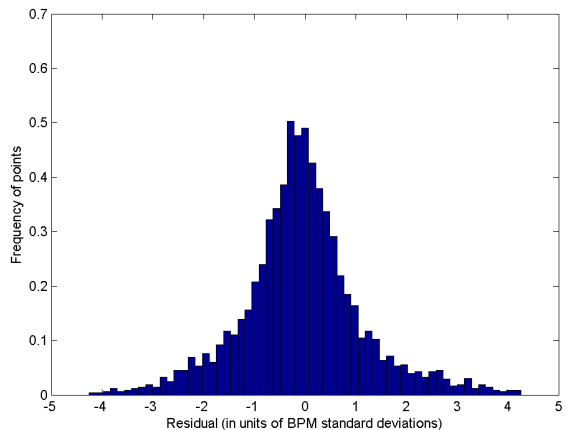

FIG. 15: Distribution of residuals from a fit using Echotek BPM data only.

V. ECHOTEK BPMS

Recent upgrade work [3] on the BPM system has equipped 20 of the ATF BPMs with digital Echotek receivers (10 in each arc). In principle, it is possible to perform a fit to the orbit response matrix and dispersion data using data from just these BPMs, since the fit will still be overconstrained. Since the correctors are distributed widely around the ring, we would expect the values of the fitted parameters to be comparable to the values obtained by fitting to data from all BPMs, even though the Echotek BPMs are concentrated in just two locations. However, performing a fit using just the Echotek BPMs would allow us to highlight the performance of these BPMs, compared to the performance of the BPM system overall.

Fig. 14 shows the standard deviation of rows and columns of the residual orbit response matrices of the

initial and fitted models to the measured orbit response matrix. Compared to Fig. 1, it appears that the residuals to the measured data are reduced when performing a fit based on data from Echotek BPMs only. This is also indicated in the distribution of residuals, shown in Fig. 15. The half-width of the distribution in units of the BPM resolution is roughly 1 ($\chi^2/N \approx 2.2$).

The gains and couplings for the Echotek BPMs, determined from the fit to the orbit response matrix using data from the Echotek BPMs only, are shown in Figs. 16 and 17 respectively. The gains show deviations of only a few percent from the ideal value. The fit using data from all BPMs (Fig. 11) suggests much larger deviations for the BPMs more generally, including the Echotek BPMs. In this respect, the results of the fit using data from the
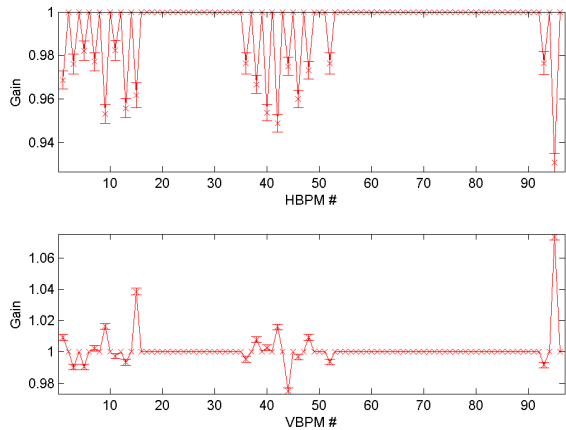
FIG. 16: Echotek BPM gains. Top: horizontal gain, g_{xx}. Bottom: vertical gain, g_{yy}. Note that in the initial model, both horizontal and vertical gain are equal to 1.

FIG. 18: Skew quadrupole integrated gradients in the fitted model, using 68 skew quadrupoles (one skew quadrupole on every sextupole).
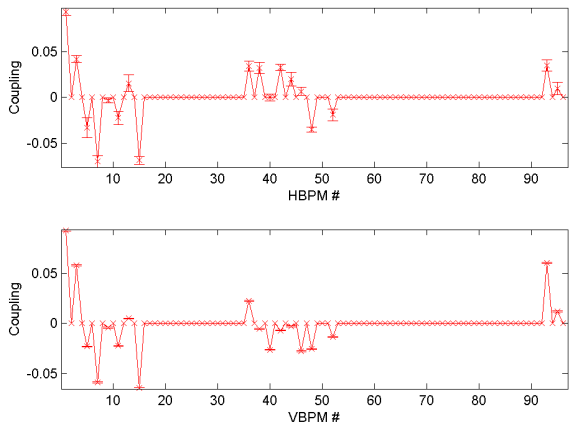

FIG. 17: Echotek BPM couplings. Top: coupling g_{xy}. Bottom: coupling g_{yx}. Note that in the initial model, both couplings are equal to 0.

Echotek BPMs only are not consistent with the results using data from all BPMs: the cause is likely to be the degeneracy between the BPM gains and the corrector strengths. This degeneracy is resolved using the dispersion data. For the fit using only Echotek BPMs, dispersion data at only the Echotek BPMs were included in the constraints, and it is possible that this was insufficient to resolve the degeneracy between the BPM gains and corrector strengths. This should be investigated further.

VI. VERTICAL EMITTANCE

Finally, we consider the skew quadrupole gradients, and the vertical emittance in the fitted models. In the initial model, the skew quadrupole gradients are zero: since ther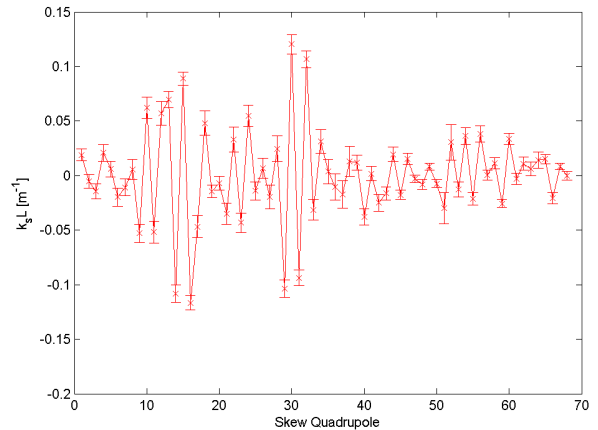e are no other sources of vertical emittance in any of the models, the vertical emittance in the initial model will be zero. Fig. 18 shows the skew quadrupole integrated gradients determined from a fit using 68 skew quadrupoles. It can be seen that there is a tendency for adjacent skew quadrupoles to take large values that approximately cancel one another.

Fig. 19 shows the skew quadrupole integrated gradients determined from fits using 34 skew quadrupoles: results from the fit using Echotek BPMs only are compared with results from fits using all BPMs with different weights on the vertical dispersion. With 34 "non-adjacent" skew quadrupoles, there is no degeneracy between the skew quadrupoles, and hence no tendency for adjacent skew quadrupoles to take large, opposite values. Also, the maximum skew quadrupole gradient is about a factor of five smaller than in the case of the fit using 68 skew quadrupoles; though, as noted above, the overall quality of the fit is not significantly worse when using 34 instead of 68 skew quadrupoles. It can be seen that there is some consistency between the results of the fit using Echotek BPM data only, and the fits using data from all BPMs.

It is interesting to calculate the vertical emittance in the fitted models. In the initial model, there is no source of betatron coupling and no vertical dispersion: therefore, the calculated vertical emittance will be zero. In the fitted model, the skew quadrupoles provide both betatron coupling and vertical dispersion. In the fitted model based on data from all BPMs and with a weight of 10 on the vertical dispersion, the equilibrium vertical emittance is around 6.5 pm; in the fitted model based on data from Echotek BPMs only, the vertical emittance is around 20 pm. Since the skew quadrupole strengths are not dramatically different between the two cases, this indicates some sensitivity of the vertical emittance to the skew quadrupole strengths.

The vertical emittance in the fitted model is also dependent on the weight given to the vertical dispersion in
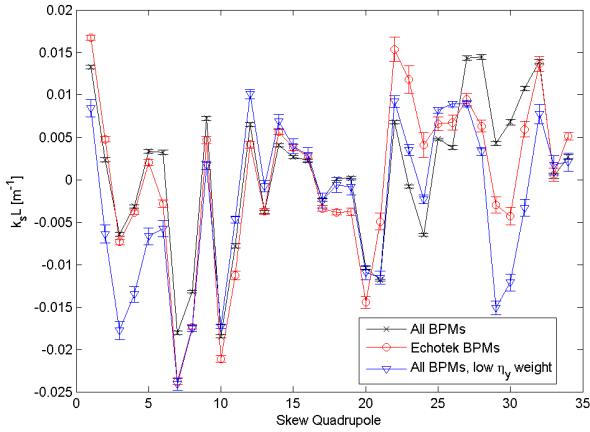
FIG. 19: Skew quadrupole integrated gradients in the fitted models, using 34 skew quadrupoles (one skew quadrupole on every SF1R sextupole only).
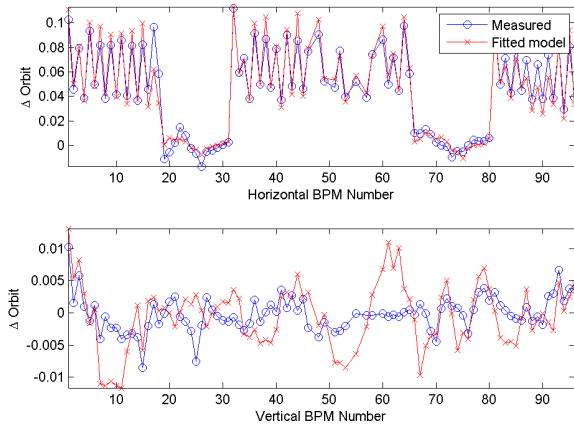

FIG. 20: Fit to "dispersion" measurement data, with a weight of 0.1 given to the vertical dispersion.

the fit. For example, repeating the fit using data from all BPMs, but with a weight on the vertical disperison of 0.1 instead of 10 results in a vertical emittance of 20 pm. The fit to the vertical dispersion data with the reduced weight is shown in Fig. 20, which should be compared to the fit shown in Fig. 6. Making this change to the weight on the vertical dispersion does not significantly affect other fitted parameters (for example, BPM gains or couplings, or normal quadrupole strengths). The beta functions and horizontal dispersion in the fitted model are also largely unaffected.

Recent measurements in the ATF damping ring indicate an equilibrium vertical emittance at low beam current of around 40 pm [13]. The fact that the fitted models predict a vertical emittance significantly less than this value suggests that it could be difficult to achieve a substantial reduction in the vertical emittance using the skew quadrupole strengths determined from the fit.
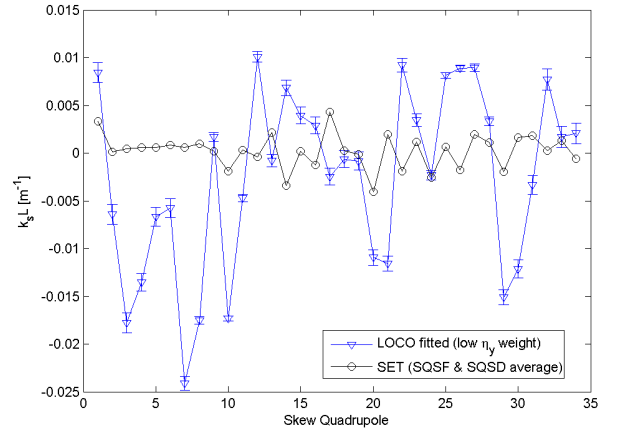

FIG. 21: Comparison between fitted and set skew quadrupole strengths. The set strengths are averaged between adjacent skew quadrupoles in each arc cell. The lack of a clear correlation suggests that coupling is dominated by vertical offset of the beam in the sextupoles.

In both fitted models, the equilibrium horizontal emittance is just under 1.4 nm.

It is possible to compare the fitted skew quadrupole gradients with those set in the machine at the time the data were taken. However, a good correlation would only be expected if the skew quadrupole strengths were the dominant source of coupling. If the coupling is dominated by vertical offset of the beam in the sextupoles, then a correlation between fitted and set skew quadrupole strengths would not be expected. A comparison between the fitted and set skew quadrupole strengths is shown in Fig. 21; the lack of a clear correlation suggests that the coupling is dominated by vertical offset of the beam in the sextupoles.

VII. CONCLUSIONS AND SUGGESTIONS

A machine model of the ATF damping ring has been fitted to recently-collected orbit response matrix and dispersion data. The model provides information on BPM parameters (gain and coupling), quadrupole strengths, and coupling. The coupling is represented as coming from the skew quadrupoles: this potentially provides data that may be used for correcting the real sources of coupling.

A comparison was made between an analysis using data from all BPMs, and an analysis using data from only Echotek BPMs. The results indicate that the Echoteks have good performance in terms of stability and systematic errors, compared to the other BPMs; this helps to achieve a good quality fit of the model to the measured data, and will likely lead to more reliable results.

Depending on how the fit to the measured data is performed, the fitted model has an equilibrium vertical emittance of between 6 pm and 20 pm. This is to be com-

pared with recent measurements of 40 pm in the ATF damping ring. Reducing the weight on the vertical dispersion in the fit seems to give a more realistic value for the vertical emittance, although the fit to the dispersion data does deteriorate somewhat. This may imply that there is a significant source of vertical dispersion in the damping ring other than coupling in sextupoles and skew quadrupoles; for example, such a source may simply be vertical steering. No vertical steering was included in the models.

We conclude that a possible approach to reducing the vertical emittance in the ATF storage ring should first attempt to correct the vertical orbit as far as possible (for example, using data from beam based alignment); and only then apply orbit response matrix analysis. More detailed simulation studies are needed to identify the op-

timum fitting parameters; in particular, the weight for the vertical dispersion. Given that the vertical emittance does appear to be reasonably sensitive to the skew quadrupole settings, achieving a vertical emittance of less than 10 pm will likely require a great deal of careful, systematic effort in measurement and tuning.

Acknowledgments

[1] J. Safranek, "Experimental determination of storage ring optics using orbit response measurements," Nucl. Inst. Meth. A388, 27 (1997).
[2] A. Wolski, M.D. Woodley, J. Nelson, M.C. Ross, S. Mishra, "Analysis of KEK-ATF optics and coupling using LOCO," ATF Internal Report, ATF-03-09 (2004). A. Wolski, M.D. Woodley, J. Nelson, M.C. Ross, "Analysis of KEK-ATF optics and coupling using LOCO," Proceedings of EPAC04, Lucerne, Switzerland (2004).
[3] M. Wendt, private communication.
[4] J. Safranek et al, "SPEAR3 commissioning," Proceedings of EPAC04, Lucerne, Switzerland (2004).
[5] C. Steier, D. Robin, A. Wolski, G. Portmann, J. Safranek, "Coupling correction and beam dynamics at ultra-low vertical emittance in the ALS," Proceedings of PAC03, Chicago, Illinois, USA (2003).
[6] M.J. Spencer, M.J. Boland, R.T. Dowd, G. LeBlanc,

Y.E. Tan, "LOCO at the Australian Synchrotron," Proceedings of PAC07, Albuquerque, New Mexico, USA (2007).
[7] http://www.slac.stanford.edu/~safranek/loco
[8] http://www-ssrl.slac.stanford.edu/at/
[9] M.D. Woodley, J. Nelson, M. Ross, J. Turner, A. Wolski, K. Kubo, "Beam base alignment at the KEK-ATF damping ring," Proceedings of EPAC04, Lucerne, Switzerland (2004).
[10] M. Wendt et al, "First ATF turn-by-turn optics measurements," ATF note (April 17, 2008).
[11] S. Kuroda et al, "Beta function measurement," ATF note (April 22, 2008).
[12] T. Okugi, S. Kuroda, K. Kubo, "Report of damping ring emittance study," ATF note (April 25, 2008).
[13] Y. Honda, "Emittance measurements with laser wire after damping ring tuning," ATF note (April 8, 2008).